Research Journal of Applied Sciences, Engineering and Technology 6(23): 4387-4392, 2013
DOI:10.19026/rjaset.6.3441
ISSN: 2040-7459; e-ISSN: 2040-7467

Submitted: January 31, 2013 Accepted: February 25, 2013 Published: December 15, 2013

Research Article

Reynolds Number Effects Investigation of Supercritical Airfoil Based on EFD and CFD

[1, 2]Da-Wei Liu, [1, 2]Xin Xu, [2]Zhi Wei and [1, 2]Yuan-Jing Wang
[1]State Key Laboratory of Aerodynamics,
[2]High Speed Aerodynamics Institute, China Aerodynamics Research and Development Center, China

Abstract: This study aimed to investigate the transonic Reynolds number effects of supercritical airfoil by EFD and CFD method. An experiment was conducted in NF-6 wind tunnel, to obtain the pressure distribution and aerodynamic coefficients of a typical supercritical airfoil through pressure measuring, with Reynolds numbers varied from 3.5×10^6 to 1.0×10^7 per airfoil chord, Mach numbers from 0.6 to 0.8, angles of attack from 0° to 8°. Also, flows over the supercritical airfoil were numerically studied; the two-dimensional Navier-Stokes equations were solved with structure grids by utilizing the Spalart-Allmaras (S-A) turbulence model, with Reynolds numbers varied from 2.0×10^6 to 50×10^6 per airfoil chord and Mach numbers from 0.6 to 0.8. Computational results compared well with experimental results. It is shown that the upper surface pressure distribution of supercritical airfoil including the location and intensity of shock wave and trailing-edge pressure coefficient, changed apparently with variable Reynolds numbers, when shock-induced trailing-edge separation existed. It is also noticed that the lift coefficient increased, drag and pitching moment coefficient decreased as Reynolds number increasing. Results implied that Reynolds number effects should be considered during the early designing stage and optimization of large aircrafts applied supercritical airfoil.

Keywords: CFD, EFD, reynolds number effects, supercritical airfoil

INTRODUCTION

For the sake of high aerodynamic efficiency, supercritical airfoil developed by Whitcomb and Clark (1965), has been widely applied to large aircrafts. This kind of airfoil has a relatively flat top, thus encouraging a weaker terminating shock wave and a region of supersonic flow with lower Mach numbers than traditional airfoils such as NACA 64 series. As a result, the value of drag-divergence Mach number will be higher for the supercritical airfoil. However, because the top of the supercritical airfoil is relatively flat, the forward 60% of the airfoil has negative camber, which lowers the lift. To compensate, the lift is increased by having extreme positive camber on the rearward 30% of the airfoil. This is the reason for the cusp-like of the bottom surface near the trailing edge (Anderson, 2010). Because of those geometry characteristics, the aerodynamic characteristics of supercritical airfoil are rather sensitive to Reynolds number at transonic conditions.

Reynolds number representing the inertia force to viscous force is one of the most important similarity parameters in wind tunnel test. The apparent difference of Reynolds number will cause the accumulated discrepancy of boundary layer equaling the change of wing geometry, which will result in different pressure distribution and affect the lift, drag and pitching moment coefficient (Liu *et al*., 2011). Therefore, Reynolds number has great effects on the economy, comfort and even safety of large aircrafts. An air accident of C-141 airplane nearly occurred during flight test for terrible prediction of lift and pitching moment acting on the wing, which results from different shock wave location brought by Reynolds number effects (Pettersson and Rizzi, 2008). However, the Reynolds number of large aircraft at flight condition cannot be simulated in normal wind tunnel except cryogenic wind tunnels such as ETW or NTF at high cost. In 1979, at that time cryogenic wind tunnels were not put into use, pressure distribution of some supercritical airfoils at flight Reynolds number were obtained through a semi-empirical method. Experimental results of low Reynolds number could be extrapolated to those of high Reynolds number with this method (Cahill and Connor, 1979). However, the stabilities of this method were not so strong that sometimes unexpected mistakes appeared; also, flow details over the airfoil could not be obtained either. Nowadays, researchers can achieve more accurate experimental results at high Reynolds

Corresponding Author: Da-wei Liu, State Key Laboratory of Aerodynamics, China Aerodynamics Research and Development Center, China, Tel.: 13404019740

number in cryogenic wind tunnels, which acquired special test model and measuring instrument, thus the penalty were long period and high expenditure (Clark and Pelkman, 2001). With the development of computer hardware's and arithmetic, CFD are playing a more and more important role in fluid dynamics research. But the numerical methods are usually used to investigation isolating from experimental results. Numerical results may be not reliable for lack of verification of experiment.

In this study, EFD and CFD were combined to investigate the Reynolds number effects of supercritical airfoil. An experiment was conducted in NF-6 wind tunnel, to obtain the pressure distribution and aerodynamic coefficients of a typical supercritical airfoil through pressure measuring, with Reynolds numbers varied from 3.5×10^6 to 1.0×10^7 per airfoil chord, Mach numbers from 0.6 to 0.8, angles of attack from 0° to 8°. As a supplementary method, verified numerical simulation was applied to predict the Reynolds effects of supercritical airfoil. Flows over the supercritical airfoil were numerically studied; the two-dimensional Navier-Stokes equations were solved with structure grids by utilizing the Spalart-Allmaras (S-A) turbulence model, with Reynolds numbers varied from 2.0×10^6 to 50×10^6 per airfoil chord and Mach numbers from 0.6 to 0.8. Typical results of the research were presented in this study.

METHODOLOGY

Wind tunnel test: An experiment was executed with variable Reynolds numbers in NF-6 wind tunnel, to investigate the Reynolds number effects of supercritical airfoil aerodynamic characteristics.

Wind tunnel and model: The NF-6 wind tunnel located in Northwest Poly-technical University of China, is capable of an absolute pressure range from 0.5×10^5 to 5.5×10^5 Pa and a Mach number range from 0.15 to 1.1 and a maximum Reynolds number of 1.5×10^7 per airfoil chord. It has a two dimensional section and a three dimensional section. The two dimensional test-section is 0.8 by 0.4 m in cross section and 3 m in length. The test section floor and ceiling are slotted (6% open) and the sidewalls are solid. The test model is a typical supercritical airfoil (Fig. 1), with 53 total pressure holes and 4 static pressure holes (Fig. 2 and 3). Rake pipe was used to measure the wake pressure, the pressure holes distribution of which could be seen in Fig. 4.

Instrumentation and test conditions: Pressure data of airfoil surface and the rake pipe were obtained with electronically scanned pressure system DSA3016, the precision of which is 0.05% F.S. The total and static pressure of wind tunnel were measured with PMP4010, the precision of which is 0.04% F.S. The total temperature was measured with MDD204, the range of which is from 263 to 373 K and the precision is 0.5 K.

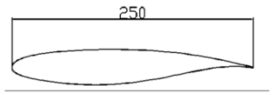

Fig. 1: Sketch of X supercritical airfoil

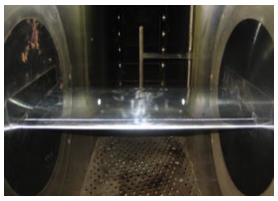

Fig. 2: Airfoil and rake pipe in 2D test section

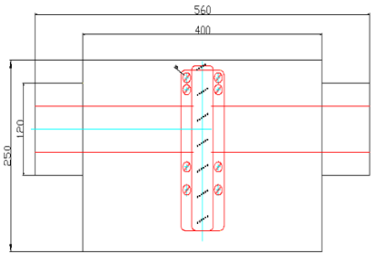

Fig. 3: Pressure holes distribution on X airfoil surface

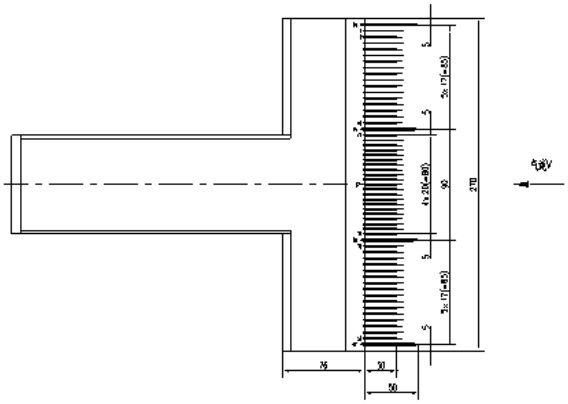

Fig. 4: Rake pipe pressure holes distribution

The pressure coefficient distribution and aerodynamic coefficients of the supercritical airfoil were obtained, through pressure testing of airfoil surface and wake, with Mach numbers varied from 0.6 to 0.8, angles of attack from 0° to 8°. Test was conducted with artificial transition located at the 7% of airfoil chord.

Data reduction: The pressure coefficient and aerodynamic coefficients of airfoil followed:

$$C_{pi} = \frac{p_i - p_\infty}{q_\infty} \tag{1}$$

$$C_L = -\oint \cos\alpha C_p d\bar{x} - \oint \sin\alpha C_p d\bar{y} \tag{2}$$

$$C_m = \left(\left[\int \bar{x} C_p d\bar{x} + \int \bar{y} C_p d\bar{y}\right) - \frac{1}{4}\int C_p d\bar{x} \quad (3)$$

$$C_D = \int_{-\frac{h}{2}}^{\frac{h}{2}} C_f(y)\frac{dy}{c} - C_{Dwt} \quad (4)$$

where, C_f (y) is the dimensionless momentum loss of the section:

$$C_f = 2\left(\frac{P_w}{P_\infty}\right)^{\frac{1}{\gamma}}\left(\frac{P_{0,w}}{P_0}\right)^{\frac{\gamma-1}{\gamma}}\sqrt{\frac{1-\left(\frac{P_w}{P_{0,w}}\right)^{\frac{\gamma-1}{\gamma}}}{1-\left(\frac{P_\infty}{P_0}\right)^{\frac{\gamma-1}{\gamma}}}}\left(1-\sqrt{\frac{1-\left(\frac{P_\infty}{P_{0,w}}\right)^{\frac{\gamma-1}{\gamma}}}{1-\left(\frac{P_\infty}{P_0}\right)^{\frac{\gamma-1}{\gamma}}}}\right)$$

where,

h : The height of rake pipe

$P_{0,w}$ & P_w : The total pressure and static pressure measured near the wake respectively

C_{Dwt} : The drag coefficient loss due to the flow of empty wind tunnel

$\bar{x} = x/c$ & $\bar{y} = y/c$: The coordinates of pressure holes to the length of airfoil chord

CFD method:

Governing equations: 2D non-dimensional Navier-Stokes equations:

$$\frac{\partial Q}{\partial t} + \frac{\partial F}{\partial x} + \frac{\partial G}{\partial y} = 0$$

where,

$$F = F_I - F_V \quad G = G_I - G_V$$

$$Q = \begin{pmatrix}\rho\\ \rho u\\ \rho v\\ E\end{pmatrix} \quad F_I = \begin{pmatrix}\rho u\\ \rho u^2 + p\\ \rho uv\\ (E+p)u\end{pmatrix} \quad G_I = \begin{pmatrix}\rho u\\ \rho uv\\ \rho v^2 + p\\ (E+p)u\end{pmatrix}$$

$$G_V = \frac{1}{\mathrm{Re}}\begin{pmatrix}0\\ \tau_{yx}\\ \tau_{yy}\\ \tau_{yx}u + \tau_{yy}v - q_y\end{pmatrix} \quad E = \frac{1}{\gamma-1}p + \frac{1}{2}\rho\left(u^2+v^2\right)$$

$$\lambda = -\tfrac{2}{3}\mu \quad \tau_{xx} = (2\mu+\lambda)u_x + \lambda v_y \quad \tau_{yy} = (2\mu+\lambda)v_y + \lambda u_x$$

$$\tau_{yy} = (2\mu+\lambda)v_y + \lambda u_x \quad \tau_{xy} = \tau_{yx} = \mu(u_y + v_x)$$

$$q_x = -\frac{\mu}{(\gamma-1)M_\infty^2 \mathrm{Pr}}\frac{\partial T}{\partial x}$$

$$q_y = -\frac{\mu}{(\gamma-1)M_\infty^2 \mathrm{Pr}}\frac{\partial T}{\partial y} \quad \mathrm{Re} = \frac{\rho_\infty u_\infty L}{\mu_\infty} \quad Ma_\infty = \frac{u_\infty}{a_\infty}$$

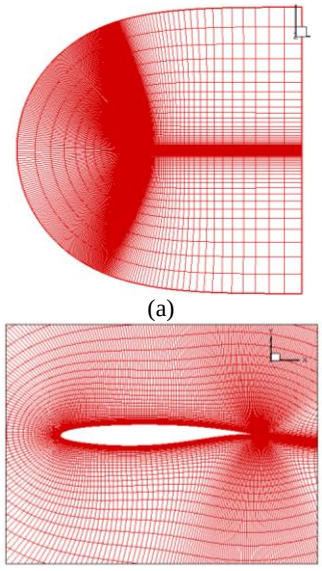

(a)

(b)

Fig. 5: (a) Overview of computational grids, (b) distribution of grids near the X airfoil wall

where, the variables with subscript 'I' represent the inviscid counterparts and variables with subscript 'V' are the viscous counterparts.

The viscous coefficient is given by Sutherland's equation:

$$\frac{\mu}{\mu_0} = \left(\frac{T}{273.16}\right)^{1.5}\frac{T+110.4}{T+110.4}$$

where, the variable μ_0 is the air viscous coefficient when temperature is 273.16 K and atmospheric pressure is 1.013×10^5 Pa.

Governing equations solution method: Spalart-Allmaras turbulence model has been mainly applied in this study while κ-ω-SST (SST) turbulence model was only for test case computation in comparison with Spalart-Allmaras turbulence model. The spatial discretization is ROE scheme and time march applies LU-SGS. Far field and wall boundary conditions have been applied to solve the governing equations in this study.

Computing model and grid: Flows over a typical supercritical airfoil X are numerically investigated in this study. As shown in Fig. 1, the upper surface of airfoil X is rather flat which delays the occurrence of shock wave and the lower surface has an aft-loaded camber compensating the loss of lift with the 250 mm airfoil chord. It is shown in Fig. 5 that structured grids have been applied. The computational grids have been generated by commercial software with a grid number about 120,000. The grid distribution on wall surface meets $y^+ = 1$. Airfoil RAE2822 for case study has the similar grid distribution.

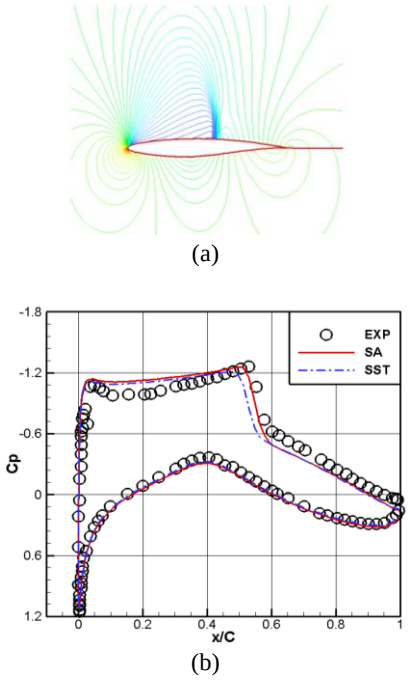

Fig. 6: (a) Pressure distribution of RAE2822 for SA turbulence model (M = 0.74, α = 4°), (b) comparison of RAE2822 pressure distribution between experimental and computational results (M = 0.74, α = 4°)

Case study: Flows over airfoil RAE2822 have been numerically solved with two different turbulence model, aimed to choose a better turbulence model, also to verify the codes applied in this study reliable in comparison with wind tunnel results. Numerical simulation has been finished under the condition that M = 0.74, α = 4° and Re = 6.5×10^6. Pressure coefficient distribution of RAE2822 shown in Fig. 6 was obtained by numerical simulation with S-A turbulence model. Comparison of computational results and experimental results has been finished. As shown in Fig. 6, computational results obtained by S-A turbulence model compare better with experimental results than those obtained by SST turbulence model, especially on capturing the shock wave location. Therefore, S-A turbulence model has been applied in this study.

Computational conditions: The computation Reynolds numbers of X airfoil vary from 2.0×10^6 to 50×10^6 per airfoil chord and angles of attack from 4° to 8° in this research when Mach numbers equal 0.74 and 0.8. Only typical results have presented in this study.

RESULTS AND DISCUSSION

Figure 7 to 9 have shown typical computational results of Reynolds number effects on pressure distribution of X airfoil, the trailing-edge pressure

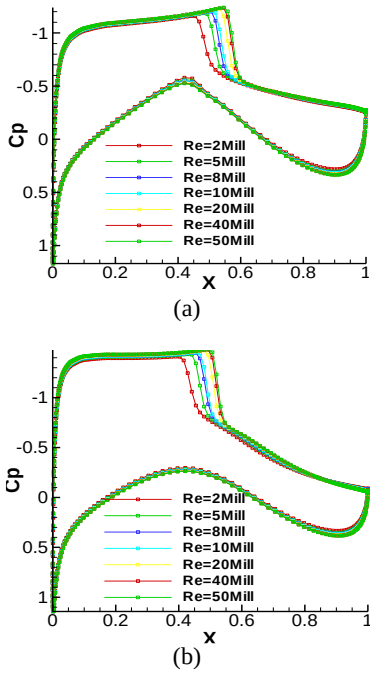

Fig. 7: (a) Reynolds number effects on pressure distribution of X airfoil at α = 4°, M = 0.74, (b) reynolds number effects on pressure distribution of X airfoil at α = 4°, M = 0.8

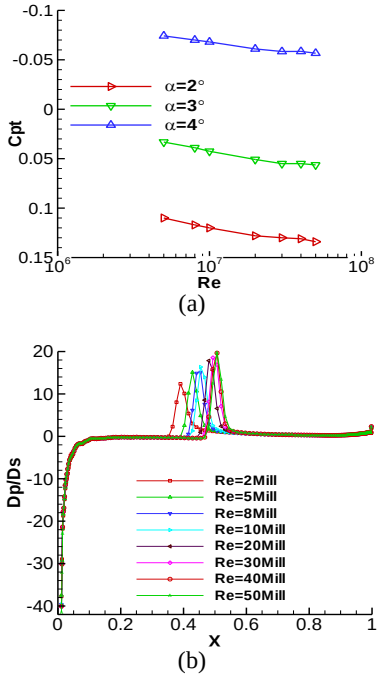

Fig. 8: (a) Reynolds number effects on training-edge pressure coefficient of X airfoil at M = 0.74, (b) reynolds number effects on pressure gradient along wall direction at α = 4°, M = 0.74

coefficient and pressure gradient along wall direction which suggests shock wave location and intensity. It can be seen that the upper surface pressure distribution

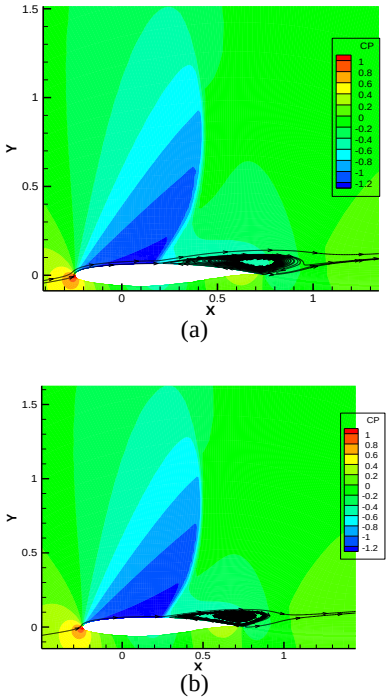

Fig. 9: (a) Reynolds number effects on the flow field around X when Re = 5×106, α = 6°, M = 0.8, (b) reynolds number effects on the flow field around X when Re = 40×106, α = 6°, M = 0.8

including the location and intensity of shock wave and trailing-edge pressure coefficient, changed apparently with variable Reynolds numbers, while the lower surface pressure distribution is not so sensitive to the Reynolds number. As the Reynolds number increases, the boundary layer of upper surface gets thinner, the location of shock wave moves afterward, intensity of shock wave increases, trailing-edge pressure coefficient improves. It is not difficult to infer that increasing Reynolds number will improve the lift and drag characteristics in a whole, also a nose down pitching moment will occur.

Curves describing the relationship of trailing-edge pressure coefficient and Reynolds number in Fig. 8 are parallel, which implies that there is some potential relationship between trailing-edge pressure coefficient and Reynolds number. The high Reynolds number trailing-edge pressure coefficient may be extrapolated from low Reynolds number trailing-edge pressure coefficient based on this relationship.

It is also evident that the Reynolds number effects are much more serious when $Re<20\times10^6$ than those when $Re>20\times10^6$. Unfortunately, the Reynolds number of experimental data obtained from ordinary wind tunnel for large aircraft is usually about 4 million while the flight Reynolds number above 30 million. It is should be noticed that the low Reynolds number wind tunnel data be corrected before utilizing it to the design of large aircraft.

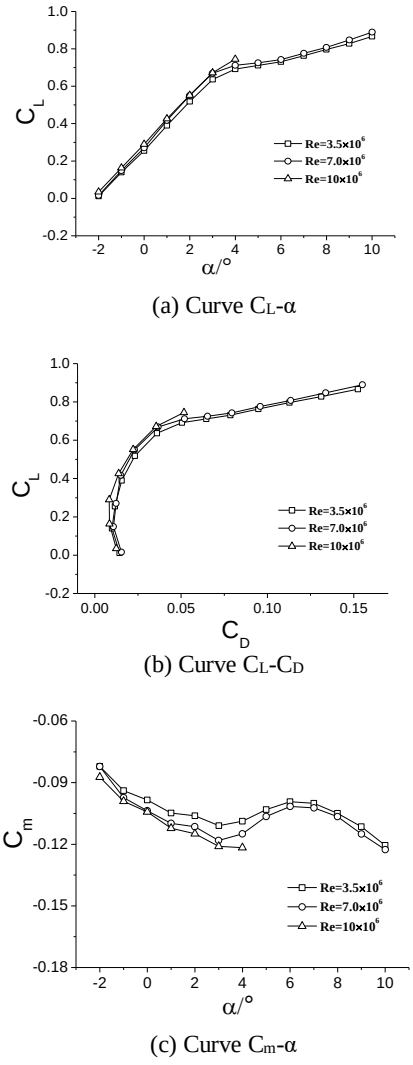

Fig. 10: Reynolds number effect on aerodynamic coefficient of YX airfoil (Ma = 0.8)

Furthermore, typical computational results of the Reynolds effects on the flow field around X airfoil have been presented in Fig. 9. It is also shown that the shock wave location moves afterward and the intensity of shock wave increases with Reynolds number increasing. As shock wave intensity strengthens, the energy loss after shock wave increases, resulting in the mechanical energy loss of shock induced training-edge separated flow, thus improving the pressure recovery characteristics after shock wave.

Experimental results of Reynolds number effects on X airfoil at M = 0.8 were given in Fig. 10. Aerodynamic coefficients were obtained through pressure integrated, the precision of which mainly depends on the distribution of the pressure holes of the rake pipe and airfoil. The integrated results indicated the Reynolds effects on the aerodynamic coefficients of the supercritical airfoil. As shown in Fig. 10, with increasing Reynolds number, the lift and the slope of

lift curve increased, also the break point delayed. The lift coefficient increased 0.034 at $\alpha = 0°$ and 0.05 at $\alpha = 4°$ respectively, with Reynolds number increasing from 3.5×10^6 to 1.0×10^7. Polar curve moves about 0.004 with increasing Reynolds number.

CONCLUSION

It is concluded that the upper surface pressure distribution changed apparently with variable Reynolds numbers, when shock-induced trailing-edge separation exists. As the Reynolds number increases, the location of shock wave moves afterward, intensity of shock wave increases, trailing-edge recovery pressure coefficient improves. Results implied that Reynolds number effects should be considered while designing and optimizing large aircrafts applied supercritical airfoil. It is possibly credible to extrapolate the low Reynolds number wind tunnel data to flight data through relations of the shock wave location, pressure recovery characteristics and Reynolds number obtained from numerical simulation.

ACKNOWLEDGMENT

The authors would like to thank the following individuals for their support of the research program, Prof. GAO Chao, ZHAO Zi-jie, PENG Xin, XU Xin, ZHOU Qiang, TAO Yang and others devoting themselves to this research.

REFERENCES

Anderson, J., 2010. Fundamentals of Aerodynamics. 4th Edn., Aviation Industry Press, UK.

Cahill, J.F. and P.C. Connor, 1979. Correlation of data related to shock-induced trailing-edge separation and extrapolation to flight Reynolds number. NASA Contractor Report 3178.

Clark, R.W. and R.A. Pelkman, 2001. High Reynolds Number Testing of Advanced Transport Aircraft Wings in the National Transonic Facility. AIAA-2001-0910.

Liu, D., D. Chen and Y. Wang, 2011. Reynolds number effect investigation of supercritical airfoil based on wind tunnel test. Syst. Simulat. Technol. Appl., 13.

Pettersson, K. and A. Rizzi, 2008. Aerodynamic scaling to free flight conditions: Past and present. Prog. Aerosp. Sci., 44: 295-313.

Whitcomb, R.T. and L.R. Clark, 1965. An Airfoil Shape for Efficient Flight at Supercritical Mach Numbers. NASA TMX-1109.